Tunable and movable liquid microlens in situ fabricated within microfluidic channels

Liang Dong and Hongrui Jiang

Citation: Appl. Phys. Lett. **91**, 041109 (2007); doi: 10.1063/1.2759469
View online: http://dx.doi.org/10.1063/1.2759469
View Table of Contents: http://aip.scitation.org/toc/apl/91/4
Published by the American Institute of Physics

Tunable and movable liquid microlens *in situ* fabricated within microfluidic channels

Liang Dong and Hongrui Jiang[a)]
Department of Electrical and Computer Engineering, University of Wisconsin-Madison, 1415 Engineering Drive, Madison, Wisconsin 53706

(Received 14 May 2007; accepted 23 June 2007; published online 25 July 2007)

The authors report on a tunable and movable liquid microlens *in situ* fabricated through fluid manipulation within microfluidics. Taking advantage of surface tensions at the microscale, the microlens is formed by a liquid droplet interfacing air. Through pneumatic control of the droplet, the microlens can be tuned in focal length and moved within the microfluidic channel on demand, thus being highly reconfigurable. A focal length tuning range from 1.5 to 8.9 mm is demonstrated. The in-plane optical axis of the microlens provides the flexibility in designing micro-optics within microfluidics, as demonstrated by realizing a planar fluorescence detection device. © *2007 American Institute of Physics*. [DOI: 10.1063/1.2759469]

Microfluidics and lab-on-a-chip systems are undergoing rapid development and have numerous promising applications. Miniaturizing optical components and integrating them into microfluidics is a profound approach to enhancing lab-on-a-chip systems, especially for biological sensing, chemical analysis, microscopic imaging, and information processing.[1–3] Recently, there have been significant advancement in integrating discrete optical components (e.g., light sources, waveguides, lens detectors, and controls) into microfluidic devices.[4–9] As an important optical component, tunable microlenses greatly benefit further miniaturization of a functionally complex lab-on-a-chip system. There are currently a few emerging tunable microlens techniques based on different mechanisms, such as electrowetting of liquid droplets, mechanical actuation of polymeric materials, and reorientation of liquid crystal.[10] However, these techniques generally require complicated microfabrication processes and various layers of materials and have little flexibility in their positions and limited reconfigurablity. Moreover, they usually have their optical axes perpendicular to the substrates, thus requiring optical alignment between multiple layers.

In this letter, we present a tunable and movable liquid microlens *in situ* fabricated through a relatively simple process by manipulating fluids within a microfluidic network. A de-ionized water droplet, segmented by air, is generated and guided to a T-shaped junction of microchannels by pneumatic fluid manipulation [Fig. 1(a)]. After surface chemistry treatment, the edges at the corners of this junction obtain high surface energy and are able to obstruct the movement of the droplet. When the air pressure difference applied to the droplet equals the internal capillary pressure caused by the curvature difference between the two liquid-air interfaces of the droplet, the liquid-air interface at the junction can protrude out of the microchannel and be steadily pinned along the edges; the shape of the other liquid-air interface, on the other hand, depends on the static contact angle of the liquid on the channel material under homogeneous pneumatic pressure. A liquid microlens is thus formed. Because of the fluidic nature of the liquid and the surface tension as a dominant force at the microscale, varying the air pressure difference within a certain range can change the shape of the pinned liquid-air interface [i.e., a change in angle θ shown in Fig. 1(a)], thus tuning the focal length of the microlens. With proper pneumatic controls, this microlens can be further moved within the microchannel, which will be discussed later.

A typical design of the microchannel network consists of a main fluidic channel, two air inlets with pneumatic pressure controls for the handling of fluids, and a lens channel [Fig. 1(b)]. This microchannel network is fabricated between two glass slides by utilizing liquid-phase photopolymerization technology.[11] First, a 450-μm-deep chamber is formed by spacing two glass slides apart with adhesive tapes. This chamber is filled with isobornyl acrylate (IBA)-based photosensitive precursor solution through the filling holes previsouly drilled in the top glass slide. This solution consists of isobornyl acrylate, tetraethylene glycol dimethacrylate, and 2,2-dimethoxy-2-phenylacetophenone in the weight ratio of 31.66:1.66:1.0. Then, the microchannels are patterned inside the chamber using a single photomask film. Exposure to a ultraviolet (UV) light source causes the prepolymer solution to harden [called poly(IBA)]. The UV light intensity and exposure time are 7.8 mW/cm^2 and 24 s, respectively. Next, ethyl alcohol is used to flush the microchannels to remove the unpolymerized precursor through the filling holes, followed by baking at 50 °C for 10 min. For the purpose of surface chemistry treatment, an octadecyltrichlorosilane (OTS) solution diluted by hexadecane [0.15% (v/v)] is flowed into the channels, and is maintained for 3 min. After that, the microchannels are cleaned by subsequently flushing 20 ml of methanol, followed by drying with a stream of nitrogen. The static water contact angle is measured on planar substrates [both poly(IBA) and glass] treated with the same OTS solution, using a goniometer, and is found to be $90 \pm 1.8°$. Hence, the resulting microlens in the rectangular microchannel is a cylindrical one whose liquid-air interface is perpendicular to the top and bottom glass substrates (see Ref. 12).

The *in situ* fabrication process of a liquid microlens is shown in Fig. 2. At the beginning, we introduce a de-ionized water stream into the main channel at an infusion rate of

a)Author to whom correspondence should addressed; electronic mail: hongrui@engr.wisc.edu.

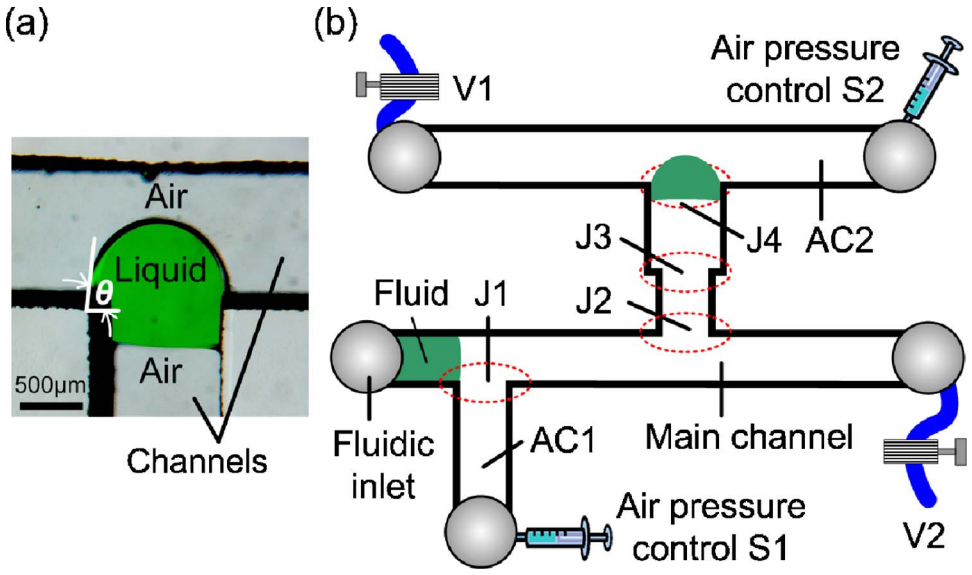

FIG. 1. (Color online) (a) Optical image of an *in situ* fabricated liquid microlens within a microchannel. The curved liquid-air interface of the microlens is pinned at a T-shaped junction. Changing the air pressure difference across the microlens can cause a change in angle θ or move the microlens from one junction to another. (b) Schematic of a microfluidic setup for the *in situ* fabrication of a liquid microlens. To realize the movement of a microlens from one junction to another, a small step is produced at junction J3.

0.5 ml/min. When the stream passes junction J1, syringe air pump S1 injects an air plug (volume: 16.2 μl; pressure: 1.013×10^5 Pa; infusion rate: 0.9 ml/min) into air conduit AC1 to separate a water droplet from the main stream. This segmented water continues to advance. When it arrives at junction J2, a lens droplet is split into the lens channel. The size of the lens droplet can be controlled by air pressures, P_1 and P_2, from air conduits AC1 and AC2, respectively. Syringe air pump S2 dispenses an air plug (volume: 10.5 μl; pressure: 1.013×10^5 Pa; infusion rate: 0.9 mL/min) into AC2 to adjust P_2. In the case of Fig. 2, the volume of the lens droplet is approximately 25% of the whole segmented water. This lens droplet subsequently advances in the lens channel, and then stops at the edges of the corners of J3 with a pressure difference $\Delta P=P_1-P_2(\sim110$ Pa) over the droplet. To sustain the microlens at these two edges, ΔP needs to be less than a critical pressure difference ΔP_C. During the fabrication of the microlens, valve V1 is closed all the time unless the microlens needs to be removed into reservoir, and V2 is opened to ambient air before a water droplet in the main channel arrives at it. The entire process is *in situ* and is completed in 10 s.

We have demonstrated that the *in situ* fabricated liquid microlens can be moved from one junction to another within the lens channel and be tuned in focal length (Fig. 3). When applying a ΔP larger than the critical pressure difference at junction J3 ($\Delta P_{J3}=215\pm2.5$ Pa), the microlens leaves J3. The lens droplet is subsequently stopped at J4 by decreasing ΔP to less than the critical pressure difference at J4 ($\Delta P_{J4}=200\pm4.5$ Pa) [Figs. 3(a)–3(d)]. The microlens at junctions (J3 and J4) can be tuned as well, while being stably pinned along the edges at the corners of the specific junction. For instance, by varying ΔP over the microlens at J4 less than ΔP_{J4}, the shape of the microlens is adjusted; for each ΔP, the microlens is able to maintain a steady state [Figs. 3(e)–3(h)]. At a ΔP larger than ΔP_{J4}, the microlens breaks the geometrical obstruction at J4 and flows into a reservoir through AC2 and V1. Figure 3(i) shows the calculated focal length of the microlens at J4 as a function of ΔP by measuring the radii of curvatures of two liquid-air interfaces of the microlens (see Ref. 12). It demonstrates that the focal length can be pneumatically controlled, varying from 1.5 to 8.9 mm over ΔP from 30 to 201 Pa. As ΔP approaches zero, f approaches infinity.

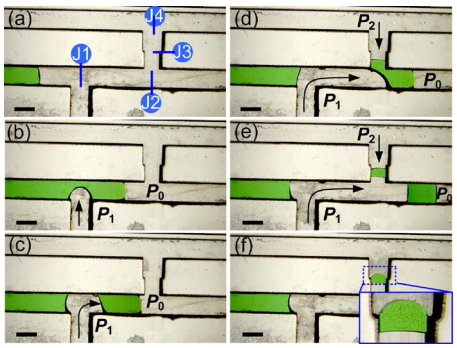

FIG. 2. (Color online) *In situ* fabrication process of a liquid microlens within a microchannel. (a) A stream is flowed into the main channel. [(b) and (c)] A water droplet is cut out of the main stream by air pressure P_1 at junction J1. [(d) and (e)] A lens droplet is split into the lens channel at junction J2. (f) The lens droplet stops at junction J3. P_0 denotes atmospheric pressure. Scale bars: 1 mm.

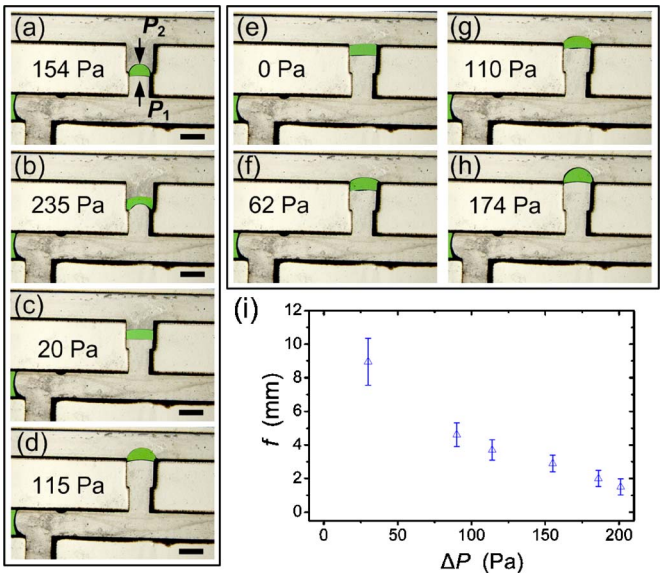

FIG. 3. (Color online) Reconfiguring an *in situ* fabricated liquid microlens. The data in each snapshot show $\Delta P=P_1-P_2$ across the microlens. [(a)–(d)] Repositioning from one junction to another. [(e)–(h)] Tuning the focal length f. (i) f at various ΔP. Scale bars: 1 mm.

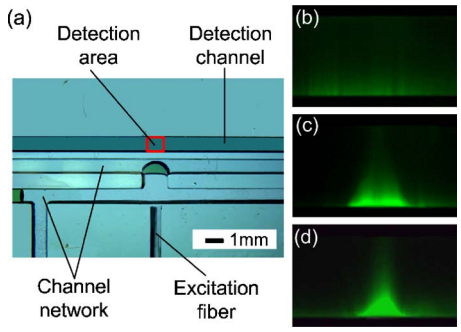

FIG. 4. (Color online) Fluorescence detection device integrating an *in situ* fabricated microlens, an optical fiber, and a detection channel on the same substrate. (a) Optical image of the device. [(b)–(d)] Fluorescence emission at the detection area in the detection channel (b) without and [(c) and (d)] with a microlens having different focal lengths. Fluorescein sodium salt: 460 nm excitation; 515 nm emission; 1 μM concentration.

The chromatic and spherical aberration inherent to the *in situ* fabricated microlens is estimated. The refractive index of water varies approximately from 1.34 to 1.33 as the wavelength of light changes from 400 to 700 nm,[13] which causes a variation of approximately 0.75% in the focal length across this spectrum. We fit the curves from the lens profiles using six order polynomials and calculate the Seidel spherical aberration coefficient using optical simulation software (OSLO-LT). The obtained spherical aberration coefficients for the microlenses at junctions J3 [Fig. 3(a)] and J4 [Fig. 3(d)] are −0.021 and −0.0175, respectively. These aberrations could be reduced by making lens combinations[9,14] or image processing.

The optical axis of our *in situ* fabricated microlens is in-plane with the microchannels. It allows for optical axes that are not limited to the ones vertical to the substrates and provides more configuration possibilities in the optical design. This microlens technology thus provides the flexibility in designing reconfigurable micro-optics within microfluidics. By combining other optical components, a single-layer infrastructure may be possible to realize complicated micro-optics that would otherwise involve multiple layers. As a demonstration (Fig. 4), we have realized a fluorescence detection device integrating a detection channel, an excitation optical fiber, and an *in situ* fabricated microlens on the same substrate. The detection channel is filled with a fluid containing fluorescein sodium salt. The excitation light is cast onto the detection channel from an external light-emitting diode through the fiber. Figures 4(b)–4(d) show the images of fluorescence emission at varying focal points of the excitation light observed through a fluorescence microscope. This demonstrates that (i) the microlens focuses the excitation light onto a specific area in the detection channel, (ii) the focused excitation light gives an increased fluorescence emission (visually stronger), and (iii) the focal point of the excitation light can be adjusted onto different locations along the width of the detection channel. It is also worthy to note that the alignment of the optical components involved in this device is defined by the pattern on the single photomask used, eliminating the need for mannual alignment.

In conclusion, we have demonstrated an *in situ* fabricated tunable and movable liquid microlens that is formed via a pinned cylindrical liquid-air interface and has in-plane optical axis. The microlens can be produced at desired locale focal lengths and be repositioned upon request, which is relatively difficult to realize by other methods. Hence it allows for unique great flexibility. The *in situ* fabrication process and planar structure possess multiple advantages, such as relatively simple fabrication process, high reconfigurability, intrinsic integration within microfluidics, and simplified system structures. A fluorescence detection device is realized by integrating this microlens, a detection channel, and an optical fiber on the same substrate. The microlens attributes (e.g., lens shape, liquid-liquid interface instead of liquid-air interface) can be configured through various parameters (e.g., cross section of lens channel, fluids used) to meet specific needs, and the microchannels can be fabricated by using other fabrication techniques, such as soft lithography with polydimethylsiloxane elastomer.[15] Although the fluid manipulation in this study is implemented pneumatically, other fluid control methods such as electrowetting[16] and photothermal control[8] could be applied to realize precise fluid manipulation. Also, using hydrophobic-hydrophilic contact lines formed via chemical surface treatments,[17] it is possible to replace the physical edges defined by the geometry of the junctions used here. We believe that this microlens technology provides great flexibility in the design and fabrication of microlenses in microfluidics and may find many lab-on-a-chip applications, such as laser-induced fluorescence detection for biological analysis.

This work was supported mainly by the U.S. Department of Homeland Security, through a grant awarded to the National Center for Food Protection and Defense at the University of Minnesota, and partly by U.S. National Science Foundation and Wisconsin Alumni Research Foundation. One of the authors (H.J.) thanks 3M Corporation (St. Paul, MN) for his Non-Tenured Faculty Award. The authors acknowledge David J. Beebe (University of Wisconsin-Madison) and his research group for fruitful discussions and access to their facilities, and Sudheer S. Sridharamurthy and Xuefeng Zeng for technical discussions and assistance.

[1] D. Psaltis, S. R. Quake, and C. Yang, Nature (London) **442**, 381 (2006).
[2] C. Monat, P. Domachuk, and B. J. Eggleton, Nature Photonics **1**, 106 (2007).
[3] R. A. Hayes and B. J. Feenstra, Nature (London) **425**, 383 (2003).
[4] Z. Li, Z. Zhang, T. Emery, A. Scherer, and D. Psaltis, Opt. Express **14**, 696 (2006).
[5] L. Dong, A. K. Agarwal, D. J. Beebe, and H. Jiang, Nature (London) **442**, 551 (2006).
[6] D. B. Wolfe, R. S. Conroy, P. Garstecki, B. T. Mayers, M. A. Fischbach, K. E. Paul, M. Prentiss, and G. M. Whitesides, Proc. Natl. Acad. Sci. U.S.A. **101**, 12434 (2004).
[7] E. Thrush, O. Levi, W. Ha, G. Carey, L. J. Cook, J. Deich, S. J. Smith, W. E. Moerner, and J. S. Harris, IEEE J. Quantum Electron. **40**, 491 (2004).
[8] G. L. Liu, J. Kim, Y. Lu, and L. P. Lee, Nat. Mater. **5**, 27 (2006).
[9] J. Seo and L. P. Lee, Sens. Actuators B **99**, 615 (2004).
[10] H. Jiang and L. Dong, Phys. World **19**, 29 (2006).
[11] D. J. Beebe, J. Moore, Q. Yu, R. H. Liu, M. L. Kraft, B.-H. Jo, and C. Devadoss, Proc. Natl. Acad. Sci. U.S.A. **97**, 13488 (2000).
[12] See EPAPS Document No. E-APPLAB-91-027729 for more fabrication and focal length estimation. This document can be reached via a direct link in the online article's HTML reference section or via the EPAPS homepage (http://www.aip.org/pubservs/epaps.html).
[13] L. Dong and H. Jiang, Appl. Phys. Lett. **89**, 211120 (2006).
[14] S. Kuiper and B. H. W. Hendriks, Appl. Phys. Lett. **85**, 1128 (2004).
[15] D. C. Duffy, J. C. McDonald, O. J. A. Schueller, and G. M. Whitesides, Anal. Chem. **70**, 4974 (1998).
[16] F. Mugele and J. C. Baret, J. Phys.: Condens. Matter **17**, R705 (2005).
[17] B. Zhao, J. S. Moore, and D. J. Beebe, Science **291**, 1023 (2001).